RevMexAA (Serie de Conferencias), **13**, 43–48 (2002)

Emission Lines from Jet Flows (Isla Mujeres, Q.R., México, November 13-17, 2000)
Editors: W. J. Henney, W. Steffen, A. C. Raga, & L. Binette

PROBING THE ORIGIN OF MASS LOSS IN T TAURI STARS

C. Dougados,[1,2] S. Cabrit,[3] and C. Lavalley-Fouquet[4]

RESUMEN

Presentamos observaciones de imágenes espectrales y de óptica adaptiva en las lineas de [O I] 6300 Å, [S II] 6716, 6731 Å y [N II] 6583 Å con el fin de restringir los posibles mecanismos de expulsión y colimación en estrellas previos a la secuencia principal. Primero analizamos observaciones de banda estrecha y alta resolución angular ($0.1'' = 15$ unidades astronómicas, UA) de los jets de CW Tau, DG Tau y RW Aur. La morfología de las regiones interiores del viento se muestran con detalles sin precedentes. Los 3 jets muestran mejor resolución que los 56 UA y muestran una anchura similar 30 UA a distancias proyectadas de $\simeq$ 100 UA. Aparentemente, el jet en DR Tau está más distorsionado, sugiriendo una fuerte interacción con el medio ambiente y/o una variación del eje del jet. Investigamos en detalle las condiciones de excitación en los microjets de DG Tau y RW Aur usando observaciones de imágenes espectrales. En ambas fuentes, los cocientes de líneas a distancias $>$ 70–100 UA se reproducen mejor usando modelos de ondas de choque, sugiriendo que variabilidad temporal juega un papel esencial a estas escalas espaciales. Sin embargo, las regiones cercanas a la fuente muestran condiciones de excitación más bajas y permanecen sin distorsiones por choques.

ABSTRACT

We present spectro-imaging and adaptive optics observations in the lines of [O I] 6300 Å, [S II] 6716, 6731 Å and [N II] 6583 Å aimed at constraining the ejection and collimation mechanisms in active pre-main sequence stars. We first discuss narrow-band high-angular resolution ($0.1''$=15 AU) observations of the jets from CW Tau, DG Tau and RW Aur. The morphology of the inner regions of the wind is revealed in unprecedented detail. All 3 jets are resolved beyond 56 AU and show similar widths of 30 AU at projected distances of $\simeq$ 100 AU. The jet in DG Tau appears more perturbed, suggesting strong interaction with the ambient medium and/or jet axis variations. We investigate in detail the excitation conditions in the DG Tau and RW Aur microjets from spectro-imaging observations. In both sources, line ratios at distances $>$ 70–100 AU are best reproduced by shock models suggesting that time variability plays an essential role at these spatial scales. The inner regions of the jets show however lower excitation conditions and may remain undisturbed by shocks.

Key Words: **LINE: FORMATION — STARS: FORMATION — STARS: PRE-MAIN-SEQUENCE — STARS: WINDS, OUTFLOWS**

1. FORBIDDEN EMISSION LINES AND T TAURI STARS

Outflow phenomena are intimately connected with the star-formation process. While the existence of a link between accretion and ejection is now well established (Cabrit et al. 1990; Hartigan et al. 1995, hereafter HEG95), the detailed physical processes involved are still poorly constrained observationally. Magneto-hydrodynamical models, where the magnetic field extracts angular momentum from the accretion process itself, provide the most consistent physical description to date (e.g., Ferreira & Pelletier 1995; Shu et al. 1995). MHD models predict that most of the collimation and acceleration processes occur over distances less than 100 AU. Constraining the physical properties of the wind at such spatial scales is thus essential to our understanding of the accretion/ejection process in young stars.

The optically-visible classical T Tauri stars (cTTs), located in the nearby Taurus cloud (d = 140 pc), offer an unique opportunity to study the mass-loss phenomenon on 100 AU scale. Indeed, although outflow manifestation is most spectacular around the younger embedded sources (ages $<$ a few 10^5 yr), the presence of substantial circumstellar material at these early stages prevents the study of the innermost regions of the wind. CTTs are typically an order of magnitude older (age $\simeq$ a few 10^6 yr) and have dissipated most of their parent gas envelope. Strong infrared excesses and blueshifted optical forbidden emission lines demonstrate that they are still actively accreting and eject-

[1]Canada-France-Hawaii Telescope Corp., Hawaii, USA.
[2]On leave from LAOG, Obs. de Grenoble, France.
[3]DEMIRM, Observatoire de Paris, France.
[4]LAOG, Obs. de Grenoble, France.

Emission Lines from Jet Flows (Isla Mujeres, Q.R., México, November 13-17, 2000)
Editors: W. J. Henney, W. Steffen, A. C. Raga, & L. Binette

ing matter, albeit at rates 10–100 times smaller than embedded sources (HEG95). The ejection/accretion rate ratio of $\simeq 0.1$ is similar in both cases, suggesting that the same driving mechanism is at work.

The forbidden emission lines were early recognized to trace the dense ($n_e \simeq 10^4$–10^6 cm^{-3}) and hot ($T \simeq 10,000$ K) central regions of the wind. It was not until the late eighties however that this conjecture was confirmed through long-slit spectroscopic observations by R. Mundt, J. Solf and their respective collaborators (Mundt et al. 1987; Solf 1994 and references therein). The systematic study by Hirth et al. (1997) confirmed the jet-like morphology of the emission, revealing spatial extensions along the jet axis of a few arcsec (up to 500 AU) in a dozen cTTs. Strong velocity and excitation gradients were observed on these scales. However, the small angular extent of the forbidden line emission regions (FLER) and their low contrast with respect to the stellar continuum (typical EW of 1 Å) prevented until recently a detailed study of the collimation and excitation processes.

We conducted between 1994 and 1998 observations at the Canada-France-Hawaii telescope with the PUEO adaptive optics system and the spectro-imaging instruments TIGER and OASIS. These two techniques, recently made available, allow one to significantly increase the line to continuum contrast and reach spatial resolutions of $0.1''$ in the optical domain. We report here on detailed studies of the FLER in three T Tauri stars: DG Tau, CW Tau, and RW Aur. We discuss the implications of these data for jet collimation and report the detection of large proper motion in the DG Tau jet in § 2. We investigate the nature of the excitation mechanism in § 3 and finally discuss in § 4 a time variable ejection model for DG Tau.

2. COLLIMATION AND TIME VARIABILITY

In 1997 we obtained with the PUEO adaptive optics system at CFHT the first [O I] 6300 Å and [S II] 6731 + 6716 Å images at $0.1''(\simeq 15$ AU) resolution of the jets in CW Tau, DG Tau, and RW Aur (see Figure 1 and Dougados et al. 2000). These images reveal for the first time the detailed morphology of the inner regions of these flows. In all three sources, the emission is resolved beyond $0.4''$ (56 AU) and shows a clear jet-like morphology with transverse FWHM ranging from 30 to 180 AU. The emission in all 3 jets appears dominated by knots.

2.1. *Collimation*

We compare in Figure 2 the measured transverse FWHM derived from *HST* observations (Ray et al.

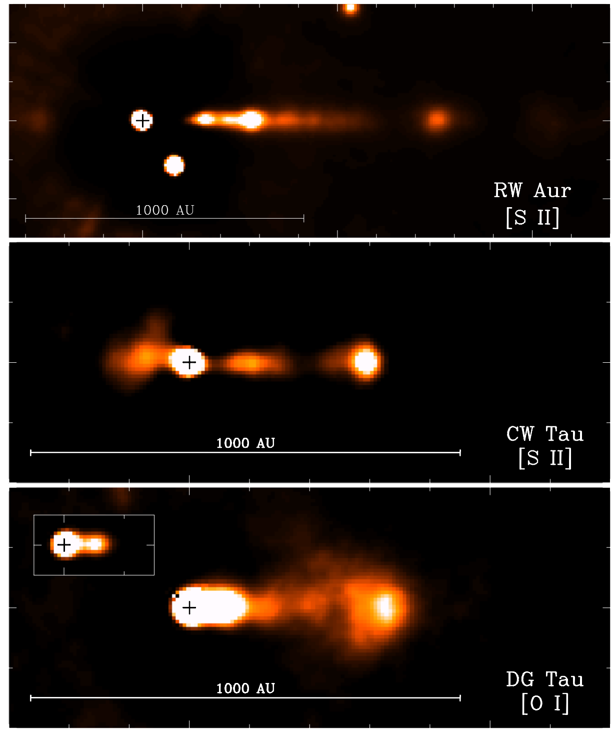

Fig. 1. Deconvolved narrow-band images of the RW Aur jet in [S II] (*top*), CW Tau jet in [S II] (*middle*) and DG Tau jet in [O I] (*bottom*). Continuum emission is also included in these maps. Resolution (after deconvolution) is $0.1''$ (pixel scale: $0.061''$). The insert in the lower panel shows the inner regions of the DG Tau jet with higher contrast. Tickmarks on the axis are shown every arcsec. The black crosses locate the centroid of continuum emission. Adapted from Dougados et al. (2000).

1996) and from our PUEO observations (Dougados et al. 2000) for the 6 jets for which we currently have measurements on similar spatial scales. These include 5 cTTs and 1 embedded source (HH 34). All 5 five jets studied so far around cTTs are resolved beyond $0.4''$ (56 AU) and show strikingly similar inner jet widths of 30 AU out to projected distances of $\simeq 100$ AU. Density collimation must therefore occur on spatial scales ≤ 56 AU, in quantitative agreement with predictions from current MHD wind models (Shang, Shu, & Glassgold 1998; Cabrit, Ferreira, & Raga 1999; see also the contribution by S. Cabrit et al. in this volume). All cTTs jets, apart from DG Tau, show in addition a similar behaviour with distance, with small opening angles of 3–4° over spatial scales of 50 to $\simeq 500$ AU. For younger, more embedded sources, driving HH flows, jet widths have been measured on the same spatial scale only in HH 34 (Ray et al. 1996). The derived HH 34 width is comparable to that observed in DG Tau where strong contamination by bow-shock wings might be

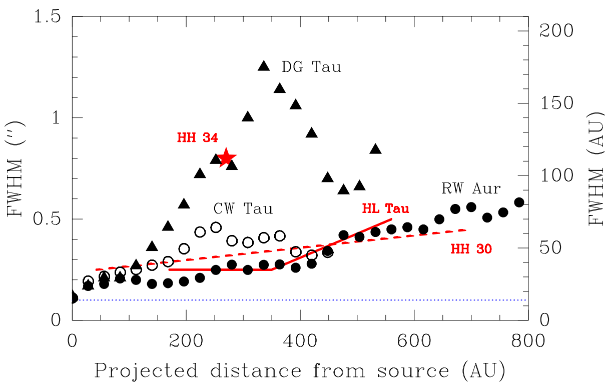

Fig. 2. Evolution of jet widths with distance. Included are our PUEO observations (symbols, labelled) as well as *HST* measurements of the HH 34 (star), HH 30 (dashed line) and HL Tau (full line) jets from Ray et al. (1996). The dotted line shows the resolution of our PUEO observations (0.1″). Adapted from Dougados et al. (2000).

present (see below), suggesting a possible evolutionary effect. It is important, however, to carry out observations of a larger sample.

2.2. *Proper Motion in the DG Tau Jet*

The outer knot in the DG Tau jet shows a clear bow-shaped morphology reminiscent of the bow-shocks observed in the younger HH flows. Comparison with the spectro-imaging data obtained 2 years earlier (Lavalley et al. 1997) reveals a proper motion of $\simeq 200$ km s^{-1} for this knot. These morphological and kinematical characteristics as well as the excitation conditions in this knot (see below) strongly suggests an internal working surface produced by time variable ejection. In addition, the DG Tau jet looks more perturbed: its FWHM increases up to 180 AU and it shows a more sinuous beam, suggesting strong interaction with the ambient medium and/or jet axis variation. We come back to this in § 3.3 below.

3. LINE EXCITATION MECHANISM

Our PUEO observations as well as the previous long-slit work by Hirth et al. (1997) have clearly demonstrated that the forbidden-line emission in T Tauri stars arises in collimated microjets detected out to a few 100 AU. A long-lasting open issue is how the jet remains hot enough to emit at these distances. Given its small launching radius, dramatic adiabatic cooling should occur in the wind expansion region and extended forbidden-line emission should not be detectable. Several heating mechanisms have been invoked for TTS microjets: (1) shocks against the disk, the environment, or within the jet itself (e.g., Hartmann & Raymond 1989; HEG95); (2) ambipolar-diffusion heating (Safier 1993a,b; Garcia et al. 2001a,b); (3) turbulent dissipation in a viscous mixing-layer (Raymond et al. 1994; Binette et al. 1999); (4) compression by jet instabilities (Bacciotti, Chiuderi, & Oliva 1995). No clear conclusion has been reached so far. Unambiguously identifying the excitation mechanism is a required step for a detailed comparison with predictions from wind models.

We present below a detailed study of the excitation conditions in the DG Tau and RW Aur microjets, based on observations obtained with the OASIS spectro-imager at CFHT in the lines of [O I] 6300 Å, [S II] 6716, 6731 Å and [N II] 6583 Å. Spatial and spectral sampling are 0.16″ and 45 km s^{-1}, respectively. We base our analysis on the following three forbidden line ratio diagnostics:

1. [S II] 6716/6731 is a well known decreasing function of the electronic density $n_{\rm e}$ for densities $\leq 2 \times 10^4$ cm^{-3}, the critical density of [S II];

2. [N II]/[O I] increases with the electronic fraction $x_{\rm e} = n_{\rm e}/n_{\rm H}$;

3. [S II]/[O I] decreases with increasing electronic temperature $T_{\rm e}$ and with increasing $n_{\rm e}$ for densities above $n_{\rm cr}$.

3.1. *Excitation Parameters*

We use the inversion method proposed by Bacciotti et al. (1995) and revised in Bacciotti & Eislöffel (1999) (hereafter BE99; see also the contribution by F. Bacciotti) to derive estimates of $n_{\rm e}$, $T_{\rm e}$, and $x_{\rm e}$ along the jet. This method assumes an optically thin homogeneous emitting region and ionization equilibrium for [O I] and [N II] ([S II] is assumed to be fully ionized). The hydrogen ionization fraction is considered as a free parameter. This method has the considerable advantage of not requiring any a-priori assumption on the excitation mechanism. However, large uncertainties are derived when strong excitation gradients are present in the emitting regions: up to 50% in $x_{\rm e}$, a factor of 2 in $T_{\rm e}$ for planar shocks with shock velocities > 50 km s^{-1}; a factor of 2 in $x_{\rm e}$ and 20% in $T_{\rm e}$ for narrow mixing layers (Lavalley 2000). Although absolute values may be uncertain, relative variations are preserved.

We apply the inversion procedure to the line ratios in the DG Tau jet, where spectral information has been divided into three velocity intervals (see Lavalley-Fouquet et al. 2000 for more details):

1. A high-velocity component (HVC), ranging from -400 to -200 km s^{-1}, highly collimated and strong in Hα and [N II].

Emission Lines from Jet Flows (Isla Mujeres, Q.R., México, November 13-17, 2000)
Editors: W. J. Henney, W. Steffen, A. C. Raga, & L. Binette

Emission Lines from Jet Flows (Isla Mujeres, Q.R., México, November 13-17, 2000)
Editors: W. J. Henney, W. Steffen, A. C. Raga, & L. Binette

2. An intermediate velocity component (IVC), ranging from -250 to -100 km s^{-1}, which traces a laterally more extended cavity and the bow-shock wings.

3. A compact but wide low-velocity component (LVC), ranging from -100 to $+10$ km s^{-1}, prominent in [O I] and [S II].

The result is shown in Figure 3, right panels. The ionization fraction $x_{\rm e}$ increases with distance at all velocities, reaching values of 60–70% at $d = 400$ AU in the HVC and IVC. A similar increase with distance has been already detected on the same spatial scales in the Th28 and HH 30 jets (BE99). In addition, $x_{\rm e}$ and $n_{\rm e}$ both increase with flow velocity. The resulting $n_{\rm H}$ decrease appears close to a d^{-2} law at distances < 280 AU.

Results of the inversion procedure for the RW Aur microjet are also shown in Figure 3, left panels. Although the RW Aur jet appears of lower excitation than the DG Tau one ($x_{\rm e} \leq 10\%$, lower densities), some of the main characteristics are recovered, namely the increase of $x_{\rm e}$ with distance and the d^{-2} decrease of $n_{\rm H}$ in the central regions ($d < 200$ AU). Also note the peak in temperature and ionization fraction at or close to the location of the first main emission peak.

3.2. *Line Ratio Model Predictions*

Figure 4, central panels, plots line ratios for three line excitation models with available quantitative predictions: planar shocks (Hartigan, Morse & Raymond 1994; HEG95), viscous mixing layers with neutral boundaries (Binette et al. 1999), and ambipolar-diffusion heated disk winds (Garcia et al. 2001a,b). Line ratios in HH objects, from the compilation of Raga, Böhm, & Cantó (1996) are also shown for comparison.

All shock models are found to follow a well-defined shock sequence in the [S II] 6716/6731 versus [S II]/[O I] diagram, while in the [N II]/[O I] versus [S II]/[O I] diagram curves for differing pre-shock densities are clearly separated. HH objects closely follow shock sequences with n_0 of 10^2–10^3 cm^{-3} as expected. Being hotter ($T \simeq 1$–3×10^4 K) and of low ionization, mixing layers separate well from planar shocks in these graphs at all but the highest densities ($n_{\rm env} \geq 10^7$ cm^{-3}). Ambipolar diffusion in disk winds establishes similar high temperatures with low ionization fractions ($< 10\%$) leading again to a clear separation from the shock model curves.

3.3. *DG Tau and RW Aur: Shocking Jets?*

In Figure 4, left and right panels, we also show the evolution of line ratios along the DG Tau and

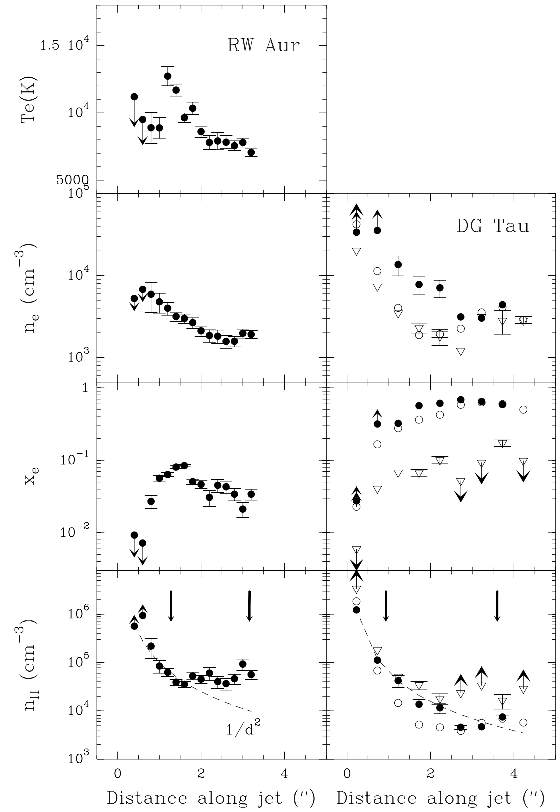

Fig. 3. Evolution of excitation parameters along the RW Aur(left) and DG Tau (right) microjets, derived using the inversion procedure of BE99. In DG Tau results are shown for the HV (filled circles), the IV (open circles) and the LV (open triangles) velocity components. In the RW Aur case, line ratios have been integrated over the range -50 to $+250$ km s^{-1}. Vertical black arrows indicate the location of the main emission knots along the jets. The dashed line illustrates a d^{-2} law for $n_{\rm H}$.

RW Aur jets respectively. In both cases, line ratios are best reproduced by shock models at all but the lowest velocities or closest distances to the star.

In DG Tau, the high [N II]/[O I] ratios observed beyond $0.2''$ clearly exclude both mixing layers with neutral boundaries and current models of MHD disk winds heated by ambipolar diffusion. Line ratios for the IVC and HVC at d $\geq 1.2''$ occupy the same regions as the densest high-excitation HH objects. Detailed comparison with the planar shock models indicate shock speeds in the range 50–100 km s^{-1} increasing with flow velocity, pre-shock densities decreasing away from the star (from 10^5 cm^{-3} at $d \simeq 30$ AU to 10^3 cm^{-3} at $d \simeq 500$ AU) and magnetic field strengths of 30–100 μG. The hypothesis of shock excitation in this source is further supported by the radial velocity jumps of $\simeq 50$ km s^{-1} observed at the location of the two bright knots along that

Emission Lines from Jet Flows (Isla Mujeres, Q.R., México, November 13-17, 2000)
Editors: W. J. Henney, W. Steffen, A. C. Raga, & L. Binette

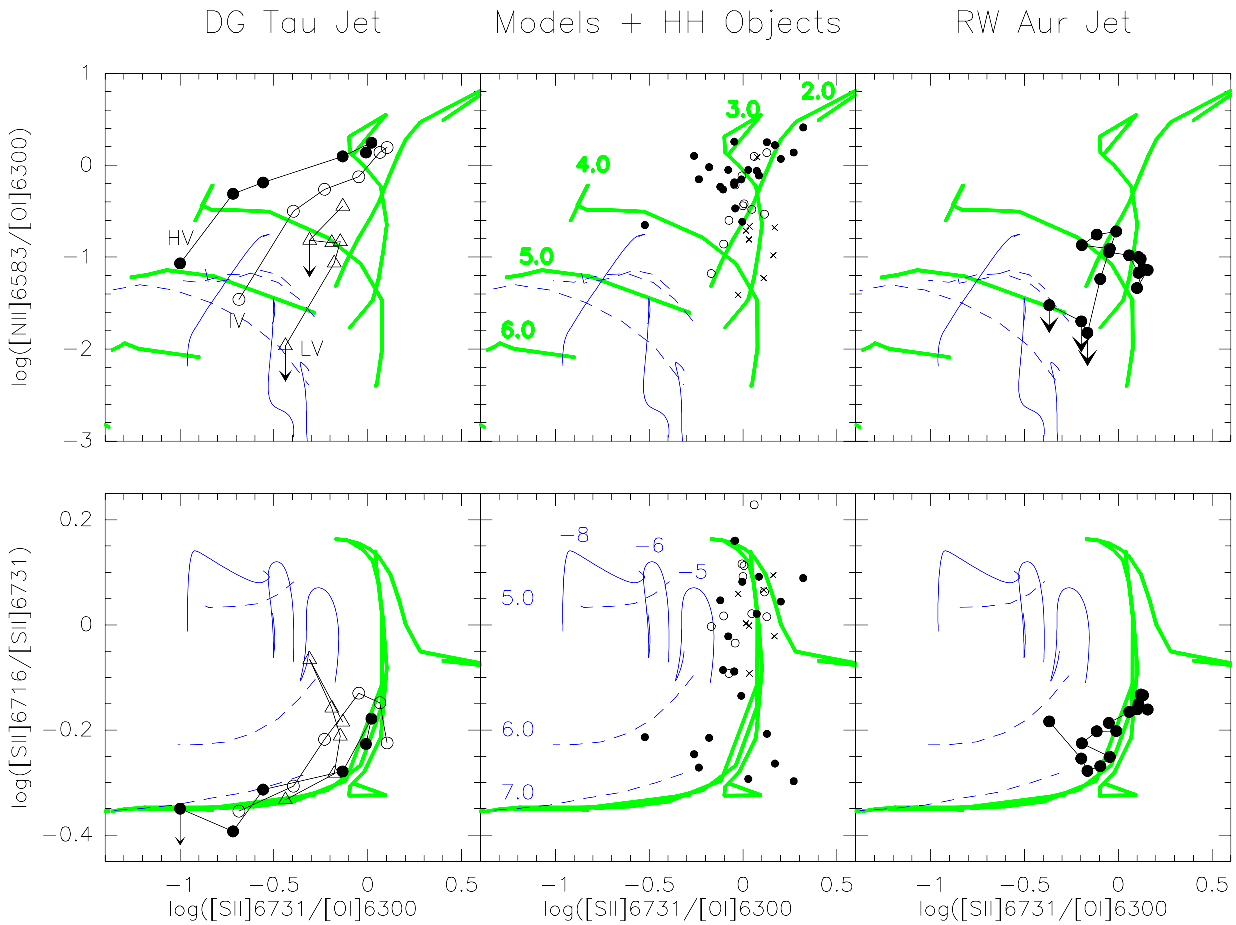

Fig. 4. Comparison of observed (symbols) and predicted (lines) line ratios. Heavy gray lines: planar shocks with $B_0 = 100\,\mu$G and $\log_{10} n_0$ as labeled on center panels. Shock speed increases with [N II]/[O I] along each curve from 15 to 100 km s^{-1}. Dashed lines: viscous mixing-layers with neutral boundaries of density $\log_{10} n_{\rm env}$ as labeled. Thin curves: ambipolar diffusion heated disk wind with accretion rates of 10^{-8}, 10^{-6} and 10^{-5} (labeled). Distance from star increases with [N II]/[O I] along each curve from 0 to 600 AU. Center panels show comparison with HH objects of high (filled circles), middle (open circles) and low (crosses) excitation. Left panels show comparison with line ratios along the DG Tau jet in the HVC, IVC and LVC velocity intervals. Points are connected with increasing distance from the star ($d = 0.2$, 0.7, 1.2, 1.7, 2.7, 3.7$''$). Right panels show comparison with line ratios along the RW Aur jet (distances along jet range from 0.2 to 3.2$''$ sampled every 0.2$''$). Adapted from Lavalley et al. (2000).

jet (see Lavalley-Fouquet et al. 2000). Furthermore, the wiggling of the faint jet beam section beyond 200 AU may signal oblique shocks between the jet and its environment. Given the jet radial velocity of -280 km s^{-1}, bends of $\simeq 10°$ would be enough to explain derived shock speeds of $\simeq 70$ km s^{-1}. The situation is somewhat reminiscent (albeit at higher density and 20 times smaller spatial scale) of the HH46/47 faint wiggling jet section, where oblique sideways shocks detected in Hα (Heathcote et al. 1996) produce large $x_{\rm e}$ of $\simeq 60\%$ (BE99). Using our inferred local shock speeds and preshock densities, we estimate a revised value of the mass-loss rate in DG Tau at d > 170 AU of 1.4×10^{-8} $M_\odot$ yr^{-1} and a lower limit to the ejection to accretion rate ratio of 4×10^{-3}.

Beyond 140 AU, line ratios in RW Aur are also most compatible with shock models. Pre-shock densities in the range 10^3 to 10^4 cm^{-3} and intermediate shock speeds of 30–50 km s^{-1} are indicated. Line ratios in the inner regions of the jet ($d \leq 85$ AU) slightly depart from the shock sequence. Lower $x_{\rm e}$ and possibly $n_{\rm e}$ and $T_{\rm e}$ are suggested there.

4. A TIME-VARIABLE EJECTION MODEL

The clear bow-shaped morphology and large proper motion of the knot at 3$''$ as well as the compatibility of the line ratios with shock models strongly support a time variable ejection for the DG Tau jet. Strong variability has been indeed observed in the high velocity wings of the emission profiles towards DG Tau: the high velocity peak of the [O I] profile has increased by 150 km s^{-1} between 1984 and 1992 (Mundt et al. 1987; HEG95; Solf & Böhm 1993). In addition, large velocity and ejection direction variations are reported for 4 outer knots (Eislöffel & Mundt 1998). The derived variability timescale is $\simeq$ 10 yrs. Similar timescales have been identified in younger HH jets such as HH 34 (Raga & Noriega-Crespo 1998). Raga et al. (2001) present a 3D hydrodynamical simulation where both the ejection velocity direction and amplitude vary with a similar period of $\simeq$ 8 yr. The morphological properties of the DG Tau line emission are well reproduced by this model but not the kinematics of the inner regions (below $1''$) suggesting that the temporal variability law is probably more complex than the assumed sinusoidal variation. Such detailed comparisons appear however very promising.

5. CONCLUDING REMARKS

From high spatial-resolution and spectro-imaging observations, we have studied in detail the collimation and excitation properties in 3 cTT jets. These observations first definitely confirm that forbidden line emission in T Tauri stars originates from the basis of HH-like jets. We derive constraints on the collimation size scale of < 56 AU and typical jet FWHM of 30 AU at 100 AU. In the 2 jets for which excitation conditions have been studied in detail (DG Tau and RW Aur) intermediate to high-velocity shocks (30 to 100 km s^{-1}) appear to be the dominant heating process beyond $d \simeq 70$ AU. Time variability may thus play a dominant role on spatial scales > 100 AU. The detailed study of a larger sample, including in particular sources without [N II] emission, is however required to test the general significance of these results. The inner regions ($d <$ 70–100 AU) may not be so strongly affected by shocks. Their study may therefore prove essential to constrain ejection models. Higher angular resolution is however required to study them in detail (see the *HST*/STIS observations of the inner regions of the DG Tau flow reported by Bacciotti et al. 2000 and Bacciotti 2002).

REFERENCES

Bacciotti, F. 2002, RevMexAA(SC), 13, 8 (this volume)
Bacciotti, F., Chiuderi, C., & Oliva, E. 1995, A&A, 296, 185
Bacciotti, F., & Eislöffel, J. 1999, A&A, 342, 717 (BE99)
Bacciotti, F., Mundt, R., Ray, T., Eislöffel, J., Solf, J., & Camenzind, M. 2000, ApJ, 537, L49
Binette, L., Cabrit, S., Raga, A., & Cantó, J. 1999, A&A, 346, 260
Cabrit, S., Edwards, S., Strom, S. E., & Strom, K. M. 1990, ApJ, 354, 687
Cabrit, S., Ferreira, J., Raga, A. 1999, A&A, 343, L61
Dougados, C., Cabrit, S., Lavalley, C., & Ménard, F. 2000, A&A, 357, L61
Eislöffel, J., & Mundt, R. 1998, AJ, 115, 1554
Ferreira, J., & Pelletier, G. 1995, A&A, 295, 807
Garcia, P. J. V., Cabrit, S., Ferreira, J., & Binette, L. 2001a, A&A, 377, 609.
Garcia, P. J. V., Ferreira, J., Cabrit, S., & Binette, L. 2001b, A&A, 377, 589.
Hartigan, P., Edwards, S., & Ghandour, L. 1995, ApJ, 452, 736
Hartigan, P., Morse, J., & Raymond, J. 1994, ApJ, 436, 125
Hartmann, L., & Raymond, J. C. 1989, ApJ, 337, 903
Heathcote, S., et al. 1996, AJ, 112, 1141
Hirth, G. A., Mundt, R., Solf, J. 1997, A&AS, 126, 437
Lavalley, C. 2000, PhD thesis, Université Joseph Fourier, Grenoble, France
Lavalley-Fouquet, C., Cabrit, S., & Dougados, C. 2000, A&A, 356, L41
Lavalley, C., Cabrit, S., Dougados, C., Ferruit, P., & Bacon, R. 1997, A&A, 327, 671
Mundt, R., Brugel, E. W., & Buehrke, T. 1987, 319, 275
Raga, A. C., Böhm, K.-H., & Cantó, J. 1996, RevMexAA, 32, 161
Raga, A., & Noriega-Crespo, A. 1998, AJ, 116, 2943
Raga, A., Cabrit, S., Dougados, C., & Lavalley, C. 2001, A&A, 367, 959
Ray, T. P., Mundt, R., Dyson, J., Falle, S., & Raga, A. 1996, ApJ, 468, L103
Raymond, J. C., et al. 1994, ApJ, 434, 232
Safier, P. N. 1993a, ApJ, 408, 115
——————. 1993b, ApJ, 408, 148
Shang, H., Shu, F., & Glassgold, A. 1998, ApJ, 493, L91
Shu, F., Najita, J., Ostriker, E., & Shang, H. 1995, ApJ, 455, L155
Solf, J. 1994, in ASP Conf. Ser., Vol. 57, Stellar and Circumstellar Astrophysics, eds. G. Wallerstein & A. Noriega-Crespo, (San Francisco: ASP), 22
Solf, J., & Böhm, K. H. 1993, ApJ, 410, L31

C. Dougados: CFHT, P.O. Box 1597, Kamuela, HI 96743, USA (dougados@cfht.hawaii.edu).
S. Cabrit: DEMIRM, Observatoire de Paris, 98 bvd Arago, 75014 Paris, France (sylvie.cabrit@obspm.fr).
C. Lavalley: LAOG, Université Joseph Fourier, 414 rue de la Piscine, F-38041 Grenoble.